Modeling a Two-section Monolithic InAs/InP Quantum-dash Laser: Wavelength Tunability and Sharp Turn-on Characteristics

M. Z. M. Khan
Optoelectronics Research Laboratory, Electrical Engineering Department, King Fahd University of Petroluem and Minerals, Dhahran 31261, Saudi Arabia

Keywords: Rate-equation Model, Tunable Laser, Broadband Laser, InAs/InP Quantum-dash Laser.

Abstract: Rate-equation based numerical model for the analysis of two-section InAs/InP quantum-dash tunable laser is developed. The model takes into account quasi-zero dimensional density of states of dashes in the linear optical gain formulation besides incorporating both homogeneous and inhomogeneous broadening of the active region. The simulation results show a broad tunability of ~22 nm from longer 2000 µm device with 700 µm absorber length compared to 1000 µm device with 300 µm absorber length, which exhibited ~15 nm tuning window, in the L-band. Moreover, a sharp turn-on behavior is also observed, which is found to be in good agreement with our recent experimental results. Such devices and their comprehensive analysis would enable design optimization of two-section quantum-dash lasers, which are promising candidates as monolithic tunable lasers for next-generation access networks.

1 INTRODUCTION

The quest to attain tunable lasers from the III-V semiconductor devices have attracted researchers to explore various configurations, aiming to enhance the tunability with a simple and cost-effective design. This thrust stems from the unprecedented application of such devices in multi-disciplinary fields such as meteorology, sensing, spectroscopy, imaging (Coldren, L. 2000, Liu, K. 2013, Pikhtin, N. A. 1997, Sheintop U. 2018), besides optical communications, particularly wavelength division multiplexed passive optical networks (Kim, A-H. 2006).

In literature, InGaAsP/InP multiple quantum-well (Qwell) active region based devices have attracted much attention for realizing monolithic tunable lasers employing multi-section structures and emitting in the C-band wavelength region. In this case, tunability was obtained by reverse biasing one of the section, or pumping the sections independently, thereby alter the absorption peak and hence the lasing wavelength (Coldren, L. 2000, Liu, K. 2013, Pikhtin, N. A. 1997). Moreover, temperature was also utilized as a control parameter (Liu, K. 2013) to achieve wavelength tuning. In general, tunability of > 10 nm has been reported from these devices. Recently InAs/GaAs quantum-dots (Qdots) based device structure has also acquired great interest as a tunable laser employing a two-section device (Feng, M. 2007) and emitting around ~1150 nm. The inherent inhomogeneous nature of the Qdots has been exploited to not only show a wavelength tunability of ~45 nm at ~1250 nm but also as a mode-locked laser (Nikitichev, D. I. et al., 2013). Very recently, InAs/InP quantum-dashes (Qdashes), which inherits the characteristics of both Qdot and Qwell nanostructures, and ability to span C- to U-band wavelengths, are also finding profound interest in myriad of multi-disciplinary field applications, as a broadband and/or externally tunable laser source (Shemis, M. A. 2018). However, owing to their much larger inhomogeneous nature, thanks to the self-assembled growth technology, a monolithic widely tunable laser would be more promising and a preferred device for practical deployment.

In this work, we propose and numerically investigated a two-section tunable InAs/InP Qdash semiconductor laser by developing a rate-equation model to understand its carrier-photon dynamics, for the first time to our knowledge. A maximum tunability of ~ 22 nm is accomplished from a 2000 µm cavity length device compared to the 1000 µm device, besides exhibiting sharp turn-on behavior. The latter characteristic is compared with our recent experimental results and found to be in good agreement. Besides, we also investigated the effect of

Khan, M.
Modeling a Two-section Monolithic InAs/InP Quantum-dash Laser: Wavelength Tunability and Sharp Turn-on Characteristics.
DOI: 10.5220/0007371901630167
In *Proceedings of the 7th International Conference on Photonics, Optics and Laser Technology (PHOTOPTICS 2019)*, pages 163-167
ISBN: 978-989-758-364-3

absorber and laser cavity length on the wavelength tunability, thus shedding light on the device design optimization requirements for eventual practical implementation.

2 NUMERICAL MODEL

The carrier-photon dynamics of a two-section InAs/InP Qdash laser is analyzed by solving a set of coupled rate equations. We group the dispersive size dashes into $j=0,1,2,\ldots\ldots 2M$ groups according to their localized interband transition energy with central energy E_{cv}, and considered $k=0,1,2,\ldots N$ intra-dash energy levels in each dash group, and characterized by their quantum wire-like density of state (DOS) function N_D (Khan, M. Z. M. 2012). We have considered three energy states of the conduction band namely; separate confinement heterostructure (SCH), wetting layer (WL), and Qdash ground state (GS), with respective carrier populations $N_{g\text{-}S}$, $N_{g\text{-}W}$, and $N_{g\text{-}j\text{-}k}$ for the gain section (length L_G), and $N_{a\text{-}S}$, $N_{a\text{-}W}$, $N_{a\text{-}j\text{-}k}$, respectively, for the absorber section (length L_A). Here $N_{j,k}$ represents the number of carriers of the j^{th} dash group with k^{th} intra-dash energy level. These carrier dynamics of different conduction band energies are separately modeled in the form of coupled rate-equations for the gain and absorber sections. In addition, a rate-equation of the photon population S_m of the m^{th} order longitudinal mode (where $m = 0,1,2\ldots.2M_p$) with mode energy E_m, of the two-section device, which is given by:

$$\frac{dS_m}{dt} = \beta\sum_{j,k} B\left(E_m - E_{j,k}\right)\left(\frac{N_{g-j,k}}{\tau_{Sp}}\right) + \frac{c}{n_a}\sum_{j,k}\Gamma\left(\left[\frac{L_G}{L}\right]gg_m^{j,k} + \left[\frac{L_A}{L}\right]ga_m^{j,k}\right)S_m - \frac{S_m}{\tau_p} \quad (1)$$

is also solved simultaneously with the other rate-equations in time-domain using fourth order Runge-Kutta method. It is worth mentioning that Eq. 1 (second term of the right hand side) along with Qdash GS rate rate-equation $dN_{g\text{-}j\text{-}k}/dt$ and $dN_{a\text{-}j\text{-}k}/dt$ couples both the gain and the absorber section carrier-photon dynamics. Here, $E_{j,k}$ represents the intra-dash energy level, weighted by Gaussian inhomogeneous broadening term $G_{j,k}$ with full width at half maximum Γ_{inh} that essentially controls the inhomogeneous broadening of the active region. The localized linear optical gain of the pumping section $gg_m^{j,k}$ and the absorber section $ga_m^{j,k}$ includes the Lorentzian homogeneous broadening term $B(E_m\text{-}E_{j,k})$, and the occupational probabilityy of the carriers at $E_{j,k}$ energy level of the dash group, are respectively given by $P_{g\text{-}jk}=N_{g\text{-}jk}/2D_gN_DV_{Ag}G_{j,k}$ and $P_{a\text{-}jk}=N_{a\text{-}jk}/2D_gN_DV_{Aa}G_{j,k}$. V_{Ag} and V_{Aa} are the associated active region volume of the gain and the absorber section, taken as 0.75 times the actual respective volume. The time constants in Eqn. 1 are the photon lifetime τ_p and spontaneous emission lifetime τ_{Sp} = 2.8 ns, whereas Γ=0.03 is the optical confinement factor.

After solving these set of rate equations for steady state solutions, the optical power at one facet can be calculated by Eq. 2 as shown (Khan M. Z. M. 2011):

$$I_m = \hbar\omega_m c S_m \ln(1/R)/(2Ln_a) \quad (2)$$

Where R is the reflectivity of the facet, n_a = 3.5 is the refractive index of the active region, L is the total cavity length and c is the speed of light (Rossetti, M. 2008, Sugawara, M. 2000). More details of other parameters can be found elsewhere (Khan, M. Z. M. 2012) and their values used in the simulation are presented in Table. 1

Table 1: Simulation parameters used in the model.

Parameter	Description	Value	Unit
d	Stripe width	3	μm
w_{WL}	Wetting layer thickness	5	nm
h_{SCH}	SCH laser thickness	100	nm
w_{Dh}	Qdash width	20	nm
h_{Dh}	Qdash height	1.5	nm
N_{hr}	Number of Qdash layers	4[a]	-
A_{eff}	Qdash effective cross-sectional area	$0.79e^{-12}$	cm^2
m^*_e	Electron effective mass	$0.04m_0$	-
$R_1=R_2$	Cleaved facet reflectivity	0.3	-
α_i	Internal modal loss	7.5	cm^{-1}
β	Spontaneous emission factor	$1e^{-4}$	-
N_D	Qdash density of states	$13e^{17}$	cm^{-3}
D_G	Qdash ground state degeneracy	1	-
D_W	WL density of states	$1.7e^{19}$	cm^{-3}
D_{SCH}	SCH density of states	$4.8e^{20}$	cm^{-3}
E_{CV}	Central transition energy	790	meV
E_{WL}	WL ground state energy	990	meV
E_{SCH}	Lowest SCH energy	1140	meV
$\hbar\Gamma_{hom}$	Homogeneous broadening	10	meV
Γ_{inh}	Inhomogeneous broadening	75	meV
τ_{SW}	Relaxation time from SCH to WL	500	ps
τ_{WS}	Re-excitation time from WL to SCH	1	ns
τ_{WD0}	Initial capture time from WL to GS	2	ps
τ_W	Recombination lifetime of WL	0.8	ns
τ_D	Recombination lifetime of Qdash	0.5	ns

3 RESULTS AND DISCUSSION

Figure 1 shows the simulated single facet optical power and the injection current (L-I) characteristics of L=1000 µm cavity single section laser device. A threshold current of I_{th} = 4.9 mA is measured with corresponding central lasing wavelength at ~1.6132 µm, as depicted in the inset of Figure 1. A total power

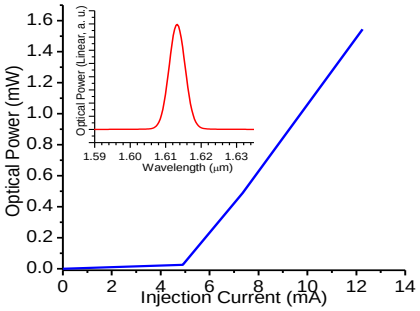

Figure 1: Simulated *L-I* characteristic of L = 1000 μm cavity length InAs/InP Qdash laser diode. Inset shows the lasing spectrum at threshold current of ~4.9 mA.

of ~1.5 mW is attained at 2.5 I_{th}. Next, we investigated the effect of absorber length on the *L-I* characteristics of the device by defining L_A/L ratio, where L_A is the absorber section length, and varying from 0.1 to 0.35. Hence, L_A/L = 0 corresponds to a single section device whose characteristics are discussed in Fig. 1. The achieved results as a function of L_A/L ratio is shown in Figure 2 alongside L_A/L = 0 for comparison purpose.A typical *L-I* characteristics is observed at small values of L_A/L up to 0.2 while a sharp turn-on behavior starts to appear at L_A/L =0.3, and appears clearer at 0.35. In other words, as the absorber section length (or absorption loss) increase within the active region, the bleaching effect, which is masking of the absorber loss of the unpumped section by the amplified spontaneous emission (ASE) of the gain section, intensifies (Le, J. and Zory, P. 2003). The threshold current is found to increase from ~4.9 mA to ~5.4 mA, ~5. 8mA and ~7.4 mA, on increasing the L_A/L ratio from 0 to 0.1, 0.2 and 0.3, respectively. Figure 2 also plots the experimentally measured *L-I* characteristics of InAs/InP quantum dash laser two-section laser. The cavity length is 930 μm with 0 V reverse bias to the absorber section, while the gain section lengths are L_G= 630 and 730 μm. Again, a sharp turn-on behavior is observed in Figure 2(b), corresponding to L_A/L = 0.25 and 0.35. This experimentally observed trend is well reproduced by the simulation results, thus showing an effective modeling of the device characteristics by the developed model (Khan M. Z. M. 2018). It is to be noted that at our objective here is to qualitatively compare the trend of Figure 2 and not to model the energy states of Qdashes accurately. Hence, a disparity in the threshold current and optical power is obvious in Figure 2 when comparing experimental and simulation results.

Figure 3 shows the effect of the absorber length on the spectral characteristics of the two section 1000 μm cavity length device, or in other words, the

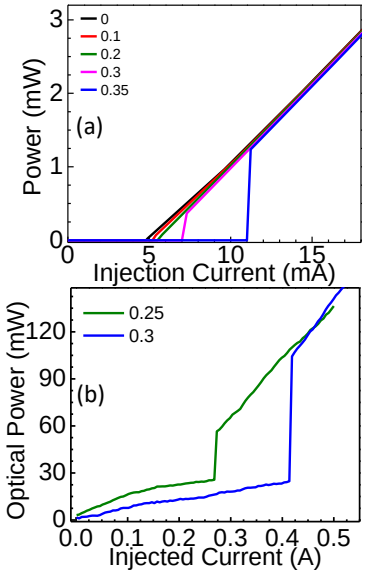

Figure 2: (a) Simulated and (b) experimental *L-I* characteristic for L = 1000 and 930 μm cavity length InAs/InP Qdash laser diode, respectively. The different absorber section length, characterized by L_A/L ratio, is shown in the legend of each figure.

wavelength tunability of the device. It can be inferred that increasing the absorber length from 100 μm to 300 μm improves the lasing wavelength tuning window of the device. A tunability of ~6.5 nm is obtained at L_A/L = 0.1 with a maximum tuning window of ~15 nm at L_A/L =0.3, corresponding to the largest absorber section length, as illustrated in Fig. 3(a). This is attributed to the additional medium loss incurred by the increase in the active region volume of the absorber section, thus requiring additional carrier and optical gain from the gain section, to compensate for the absorption loss. This basically blue shifts the lasing spectrum as the carrier continuously occupy higher energy states. For L_A/L > 0.2, a saturation of wavelength sift is observed. It is to be noted that the absorber section is left open in the simulation while the gain section is pumped with current to achieve lasing from the two-section device.

Fig. 3(b) shows the corresponding lasing spectrums at 1.05$I_{th.}$ Besides blue shifting, broadening of the lasing bandwidth is also observed on increasing the absorber section length. This might again be ascribed to carrier filling of more inhomogeneous dash states. In other words, more dispersive states are exposed wherein carrier are occupied to compensate from the high losses at large L_A/L ratio, thus broadening the lasing spectrum. Nevertheless, a proper optimization of the L_A/L ratio enabled achievement of wide tunability covering L-band wavelength region (~1.6132 to ~1.5983 μm).

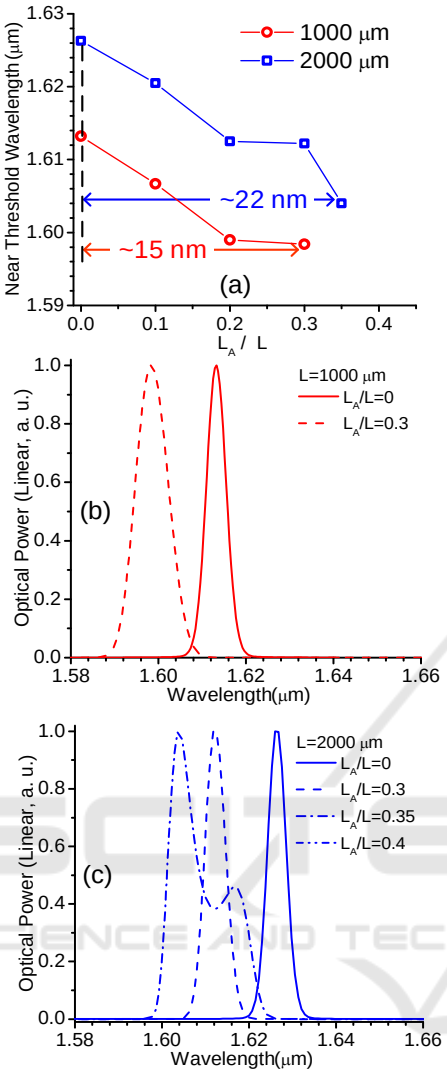

Figure 3: Simulation results of the (a) effect of the ratio of absorber length to total cavity length (L_A/L) on the tunability of the InAs/InP Qdash laser at L = 1000 μm and 2000 μm cavity lengths. (b) and (c) are the corresponding near threshold (1.05I_{th}) lasing spectrums. Note that the absorber section was left open while the gain section was pumped to achieve lasing from the device.

Next, the effect of cavity length on the tuning window of InAs/InP Qdash laser is investigated by presenting the results of L=2000 μm cavity device in Figure 3(a). A similar trend in the wavelength tunability is observed from the longer device with saturation of wavelength shift between $0.2 \leq L_A/L \leq 0.3$, compared to the shorter cavity device. A considerably shift of ~8 nm from L_A/L = 0.3 to 0.35 is observed thereafter. Moreover, the near threshold lasing wavelength, in this case, depicted in Figure 3(c), shows a broad lasing spectrum below the -3dB bandwidth, with a single facet power of ~0.6 mW, thus exhibiting a discontinuity in the *L-I* curve (Feng, M. et al., 2007). We postulate that these are the signature of excessive absorption in the active region, leading to stimulated emission with high power and broad bandwidth just above threshold (Feng, M. et al., 2007). Nonetheless, the lasing wavelength is blue shifted, thus contributing to a total tunability of ~22 nm.

The proposed two-section InAs/InP device is discretely wavelength tunable, whose resolution is dictated by the longitudinal mode spacing of the laser cavity length. Moreover, wavelength tuning within the tunable window could be easily accomplished by pumping the absorber region. For instance, a current with value between > 4.9 mA and < 7.4 mA is required to obtain various tunable wavelengths for L_A/L = 0.3 device, which could be obtained by a variable resistor at the absorber section. Lastly, at above threshold pumping current (> 1.5I_{th} - 2.0I_{th}) of the gain section, similar behavior of the wavelength tunability is observed at various L_A/L ratio except the lasing spectrum -3dB bandwidth is observed to be broad reaching as large as ~10-30 nm.

4 CONCLUSION

In summary, a rate-equation numerical model for the analysis of two-section tunable InAs/InP Qdash laser device was developed and applied to study the effect of absorber section and cavity length on the device tunability. The results show a larger absorber length of 700 μm attain wider tunability of ~22 nm in the L-band from a longer 2000 μm cavity length device. Moreover, a sharp turn-on behaviour in L-I characteristics is also noted, in line with the experimental observation. These findings could provide a guidance for device design optimization to achieve maximum possible tunability from the compact and simple monolithic tunable laser, which is a potential candidate for the next generation optical access networks.

ACKNOWLEDGEMENTS

This work was supported by Deanship of Research, King Fahd University of Petroleum and Minerals, through grant no. IN161029. The author gratefully acknowledge contributions from Emad Alkhazraji from KFUPM and Mohd. Sharizal Alias from

KAUST, for heling with the experimental results and the device fabrication, respectively.

REFERENCES

Coldren, L. et al., 2004. Tunable semiconductor lasers: A tutorial. *Journal of Lightwave Technology*, 22(1).

Feng, M., Brilliant, N. A., Cundiff, S. T., Mirin, R. P., Silverman, K. L., 2007. Wavelength bistability in two-section mode-locked quantum-dot diode lasers. *IEEE Photonics Technology Letters*, 19(11), pp.804-806.

Khan, M. Z. M., Ng, T. K., Schwingenschlogl, U., Ooi, B. S., 2012. Spectral analysis of quantum-dash lasers: effect of inhomogeneous broadening of the active-gain region. *IEEE Journal of Quantum Electronics*, 48(5), pp. 608-615.

Kim, A-H., Park, J-H., Cho, H-S., Lee, C-H., 2006. Laser spectral envelope control using a double contact Fabry-Perot laser diode for WDM-PON. *IEEE Photonics Technology Letters*, 18(20), pp.2132-2134.

Liu, K., Mu, S. X., Lu, Y., Guan, B. L., Pun, E. Y. B., 2013. L-Band Wavelength-Tunable MQW Fabry–Pérot Laser Using a Three-Segment Structure, *IEEE Photonics Technology Letters*, 25(18).

Nikitichev, D. I. et al., 2013. High-power wavelength bistability and tunability in passively mode-locked quantum-dot laser. *IEEE J. Sel. Top. Quantum Electron.*, 19(4), pp. 1100907.

Pikhtin, N. A. et al., 1997. Two-section InGaAsP/InP Fabry-Perot laser with a 12 nm tuning range. *Technical Physics Letters*, 23(3), pp.214-216.

Rossetti, M., Bardella, P., Montrosset, I., 2008. Numerical investigation of power tunability in two-section QD superluminescent diodes. *Optical and Quantum Electronics*, 40(14), pp. 1129-1134.

Shemis, M. A., et al. 2018. Broadly Tunable Self-injection Locked InAs/InP Quantum-dash Laser Based Fiber/FSO/Hybrid Fiber-FSO Communication at 1610 nm. *IEEE Photonics Journal*, 10(2).

Sugawara, M., Mukai, K., Nakata, Y., Ishikawa, H., Sakamoto, A., 2000. Effect of homogeneous broadening of optical gain on lasing spectra in self-assembled $In_xGa_{1-x}As/GaAs$ quantum dot lasers. *Physical Review B*, 61(11), pp. 7595.

Le, J. and Zory, P. 2003. Sharp turn-on diode lasers. *In 16th Annual Meeting of the IEEE Lasers and Electro-Optics Society (LEOS).* 2. pp. 987-988.

Khan M. Z. M., Ng T. K., Schwingenschlogl U., Ooi B. S. 2011. Effect of the number of stacking layers on the characteristics of quantum-dash lasers. *Optics Express*, 19(14).

Khan M. Z. M. 2018. Tunable Two-section InAs/InP Quantum-dash Laser: Numerical Modeling and Analysis. *IEEE Photonics Journal*, 10(6).

Sheintop U., Perez E. and Noach S. 2018. Narrow Bandwidth Tunable Watt Level Tm:YAP Laser using Two Etalons. In Proceedings of the 6th International Conference on Photonics, Optics and Laser Technology - PHOTOPTICS, pp. 303-307.